Eurasian Chem.-Technol. J. 27 (2025) 139–148
The journal of the Institute of Combustion Problems https://ect-journal.kz

https://doi.org/10.18321/ectj1661

Effect of the Various Delignification Methods on the Individual Lignin Pyrolysis Products

S.A. Pokryshkin, Yu.A. Sypalova, I.A. Grishanovich, A.Yu. Kozhevnikov*

Core Facility Center "Arktika", Northern (Arctic) Federal University named after M.V. Lomonosov, Northern Dvina Emb., 17, Arkhangelsk, 163002, Russia

Article info

Received:
9 October 2024

Received in revised form:
25 December 2024

Accepted:
24 February 2025

Keywords:
Lignin
Monomeric composition
Thermal destruction
Py-GC/MS

Abstract

Pyrolysis-gas chromatography-mass spectrometry (Py-GC/MS) was used to analyze a series of the technical and near-native birch lignins. The main monomeric components of lignins and their ratios have been determined. The contribution of the main monomeric units (S/G/H) to the lignin macromolecule was evaluated. Structural fragments are shown, the content of which is significantly influenced by the delignification method. Using RDBE (ring double bond equivalents) vs C_n and van Krevelen diagrams allowed to comprehensively characterize the monomeric composition of lignin pyrolysis products. Differences in the structure of all lignins, depending on the method of delignification, were visualized using principal component analysis (PCA). Hierarchical cluster analysis (HCA) allowed to divide studied lignins into three distinct groups: low-modified/near-native (milled wood lignin); moderately modified (alkaline ethanol lignin, soda lignin); and highly modified (kraft lignin, hydrolysis lignin, dimethyl sulfoxide lignin). The application of Py-GC/MS combined with chemometric techniques provides detailed information on changes in the lignin structure, depending on the degree of severity of the delignification process.

1. Introduction

Lignin is a complex polymer that is the main structural component of plant cell walls. Lignin primarily provides rigidity to cell walls, playing a crucial role in maintaining the plant shape [1]. It also has an antimicrobial effect, helping to protect plants from harmful microorganisms [2]. Furthermore, lignin is a major byproduct in the pulp and paper industry (PPI) [3]. Approximately 100 million tons of lignin are currently produced annually as a PPI byproduct [4]. The largest amount of technical lignin is produced during sulfate (kraft) pulping (ca. 85% of the total lignin production) [5, 6]. The great potential for high-value utilization of lignin lies in its abundance of aromatic compounds [7]. However, the difficulties in extracting individual components and the lability of lignin structure determined its main use for heat recovery, resulting in low-value utilization [8]. Extracting aromatic compounds from lignin is a complex process, but the lignin-first strategy is a crucial approach for highly efficient for biorefining [9, 10]. The structure of technical lignins depends on both the botanical origin of the feedstock [11] and its processing conditions, particularly related to the delignification process [12]. One of the main factors that worsens lignin structure is condensation. This process is directly proportional to the severity factor of the delignification conditions [13, 14].

A detailed characterization of lignin structure is required to develop effective strategies for its further processing. The ratio structural units of lignin monomers (S:G:H) is one of the main characteristics of a technical lignins [15], and it is no less important for assessing native lignin, as the content of monomeric units depends on the type of plant biomass [16]. Pyrolysis-gas chromatography/mass spectrometry (Py-GC/MS) is widely used to quantify syringyl (S), guaiacyl (G) and p-hydroxyphenyl (H) units of lignins [17-19]. Py-GC/MS has the advantages of using a rapid, inexpensive and rather accurate analytical method [20]. The essence of the approach is that, during pyrolysis, lignin decomposes into smaller

*Corresponding author.
E-mail address: akozhevnikov@mail.ru

fragments, which are then identified and compared. We have previously shown that the pyrolysis process conditions affect the composition and quantitation of the lignin structural units [21]. Other researchers have used this method to study the composition of the bark and wood of *Toona sinensis* [22].

In order to estimate the impact of different delignification methods on lignin structure, we have excluded the influence of the botanical origin of feedstock in this study. Therefore, by studying one wood species, the influence of delignification methods on the ratio of lignin monomeric units can be determined. The contribution of each individual monomeric unit to the S:G:H ratio depends on the specific pyrolysis products [23]. The study of these products makes it possible to accurately determine the dependence of lignin destruction and modification on treatment methods of lignin-containing feedstocks.

Thus, this work is based on an assessment of changes in lignin structure under different delignification methods, through the study of its monomeric pyrolysis products.

In studying the effect of delignification methods on lignin structure, it is important to visualize Py-GC/MS data sets obtained for each sample in order to identify differences and correlations. Chemometric analysis is a promising way to visualize variations within large multivariate datasets. In particular, principal component analysis (PCA) and hierarchical cluster analysis (HCA) provide a comprehensive overview of systematic variations in complex data [24]. In addition, these chemometric methods have been proven effective in the analysis of data from lignin structural research [25]. The application of Py-GC/MS combined with chemometric techniques can provide detailed information on changes in the lignin structure, depending on the severity of the delignification process.

This work studies the structure of technical and near-native birch lignins by investigating the monomeric composition during pyrolytic decomposition.

2. Experimental

Silver birch xylem (*Bétula pendula*) was used as the feedstock for delignification. The 40-year-old wood was harvested in the Arkhangelsk forestry. The xylem was ground using an analytical knife mill. The extractives were removed by 16-hour reflux with acetone in a Soxhlet apparatus. The chemical composition of the original birch wood has been determined as previously described [23] and is presented in Table S1. The extractive-free birch sawdust was then delignified in different ways.

2.1 Isolation of lignins

The following lignin preparations were extracted: hydrolysis lignin (Hyd-L) [26], sulfate/kraft lignin (Kraft-L) [27], soda lignin (Soda-L) [28], dimethyl sulfoxide lignin (DMSO-L) [23], alkaline ethanol lignin (SodaEt-L) [21], dioxane lignin (DL) [21], and milled wood lignin (MWL) [21], according to previously reported protocols. Detailed instructions on lignins isolation can be found in the “Supplementary Information” file.

2.2 Py-GC/MS

Pyrolysis was performed according to the previously established mode [21]. For the pyrolysis of the studied set of lignins, a temperature of 400 °C was used. This is due to the presence of highly modified lignin samples, which emit low amounts of monomeric pyrolysis products. The Py-GC/MS analysis was performed using a QP2010 Plus (Shimadzu, Japan) gas chromatograph-mass spectrometer equipped with an EGA/PY-3030D pyrolyzer (Frontier Laboratories Ltd., Japan).

The pyrolytic oven temperature was programed from 50 to 400 °C at a rate of 120 °C/min, with a 1 min holding time at the final temperature. GC/MS analysis was performed using a HP-5MS fused-silica capillary column (30 m × 0.25 mm i.d., 0.25 µm f.t.) with a temperature gradient from 40 to 202 °C at a heating rate of 3 °C/min followed by a post-run program at 320 °C for 3 min, with a split ratio of 1:20. MS detection was performed in a mass range of 15-500 Da, at a scan rate of 5 spectra/sec. The composition of monomeric pyrolysis products was identified using NIST and Wiley databases.

The lignin samples were powdered by grinding in an agate mortar before pyrolysis. The sample weight ranged from 85 to 125 µg. Pyrolysis of each lignin preparation was performed in triplicates.

2.3 Chemometric analysis

The obtained Py-GC/MS data were subjected to Hierarchical Cluster Analysis (HCA) and Principal Component Analysis (PCA) using Origin® 2019b software (OriginLab Corporation, US).

Hierarchical cluster analysis (Fig. 1) is a method of mathematical data processing that uses an algorithm to identify patterns and similarities in data. It involves grouping similar data points and creating clusters of data. This method uses pairwise distance information to create a dendrogram that rearranges data tables in a hierarchical structure [29].

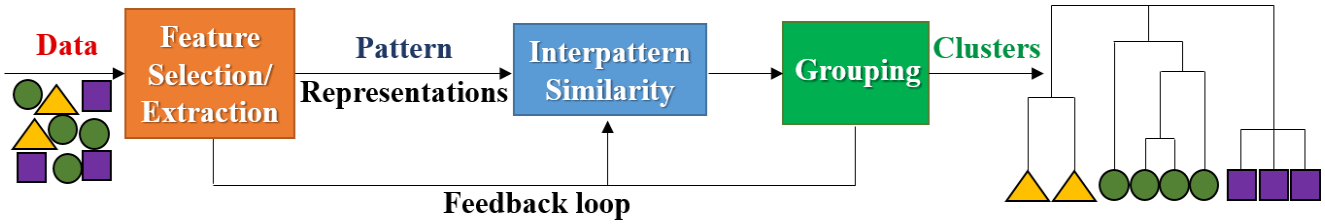

Fig. 1. HCA scheme.

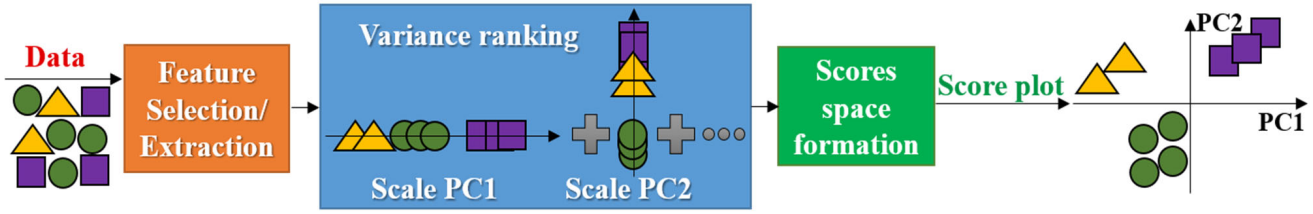

Fig. 2. PCA scheme.

Principal component analysis (Fig. 2) is a statistical method used to analyze and visualize complex datasets. It identifies the most significant patterns or features in the data and then projects them onto a new set of variables. It allows us to trace variations in the data at different levels. It is possible to group data samples with similar characteristics and identify possible outliers [24].

During data processing by the PCA method, a correlation matrix and listwise parameters were used. During data processing by the HCA method, the group average method and the Euclidean distance type were used. The number of clusters was determined experimentally. Score plots, loading plots, and dendrograms from the cluster analysis were generated.

Ring double bond equivalents (RDBE) is a measurement of unsaturation. RDBE was calculated according to Eq. 1:

$$RDBE = C - (H/2) + (N/2) + 1 \quad (1)$$

where C, H, N are the number of carbon, hydrogen and nitrogen atoms in the molecule, respectively.

The RDBE for the entire lignin preparation was calculated as the sum of the RDBEs of the identified pyrolysis products, multiplied by the relative area of each compound's peak.

3. Results and discussions

3.1 The study of lignin pyrolysis products

Py-GC/MS pyrograms of all the studied lignins have been obtained. An example of such a chromatogram is shown in Fig. 3. The retention times of some phenolic pyrolysis products are presented in Table 1. A detailed analysis of the chromatograms revealed 30 major monomeric pyrolysis products. These included 5 compounds corresponding to the H-units of lignin, 10 compounds corresponding to G-units, 12 compounds corresponding to S-units, and 3 compounds with a polyhydroxyaromatic (PolyOH) structure (Table S2). The peak areas of the identified monomers were normalized by the weight of the lignin sample and averaged between replicates.

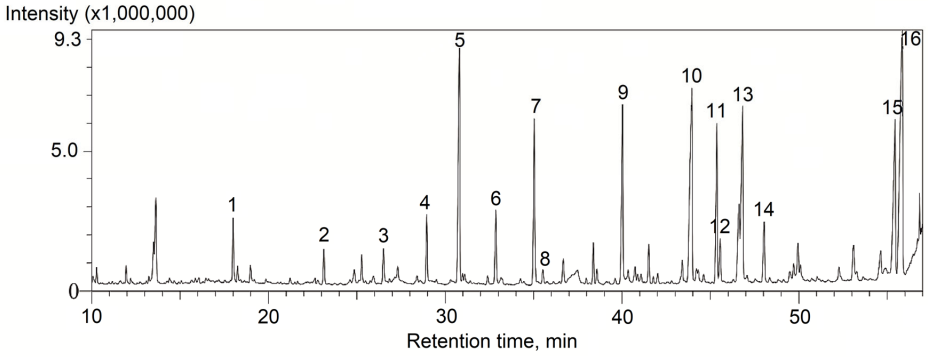

Fig. 3. Chromatogram of the MWL pyrolysis products.

Table 1. Some identified compounds and their retention times

Peak No	Rt, min	Name
1	18.022	Phenol, 2-methoxy (Guaiacol)
2	23.161	Phenol, 2-methoxy-4-methyl (Methylguaiacol)
3	26.501	Pyrogallol 1-methyl ether (Methoxycatechol)
4	29.002	2-Methoxy-4-vinylphenol (Vinylguaiacol)
5	30.822	Phenol, 2,6-dimethoxy (Syringol)
6	32.867	Benzaldehyde, 4-hydroxy-3-methoxy (Vanillin)
7	35.048	Phenol, 4-methyl, 2,6-dimethoxy-(4-methylsyringol)
8	35.549	Phenol, 2-methoxy-4-propyl (Propylguaiacol)
9	40.085	Phenol, 4-ethenyl, 2,6-dimethoxy-(4-vinylsyringol)
10	43.858	Benzaldehyde, 4-hydroxy-3,5-dimethoxy (Syringaldehyde)
11	45.361	Phenol, 2,6-dimethoxy-4-(2-propenyl)-(4-Propenylsyringol-)
12	45.597	1-(4-Hydroxy-3,5-dimethoxyphenyl)-ethanal (Homosyringaldehyde)
13	46.77	2-Propen-1-ol, 3-(4-hydroxy-3-methoxyphenyl) (Coniferyl alcohol)
14	48.064	1-(4-Hydroxy-3,5-dimethoxyphenyl)-2-propanone (Syringyl acetone)
15	55.397	(E)-3-(4-hydroxy-3,5-dimethoxyphenyl) prop-2-enyl (Sinapyl aldehyde)
16	55.773	2-Propen-1-ol, 3-(4-hydroxy-3,5-dimethoxyphenyl) (Sinapyl alcohol)

Table 2. Lignin structural units content, %

	MWL	DL	SodaEt-L	DMSO-L	Kraft-L	Soda-L	Hyd-L
H	0.5±0.0	0.3±0.0	0.4±0.0	0.8±0.0	0.7±0.0	0.6±0.0	2.1±0.1
G	29.4±0.5	28.7±0.4	34.7±0.2	36.4±0.1	35.0±0.3	30.9±0.1	31.7±0.3
S	67.7±0.6	69.1±0.4	62.0±0.1	59.5±0.1	60.1±0.3	63.5±0.2	59.9±0.4
PolyOH	2.4±0.1	1.9±0.0	2.9±0.1	3.3±0.0	4.2±0.1	5.0±0.1	6.0±0.4

Based on the monomeric composition and peak areas, the percentage of lignin structural units were calculated (Table 2). According to Table 2, the number of monomeric units in lignin varies depending on the delignification method. Near-native birch lignins, such as milled wood lignin (MWL) and dioxane lignin (DL), have a higher content of syringyl units (~ 70%) and fewer guaiacyl units (~ 30%). Hydrolysis lignin (Hyd-L) significantly differs from other samples due to its high content of PolyOH and hydroxyphenyl (H) structural units, and low amount of syringyl (S) units.

Then, the contribution of each individual component to the S/G/H ratio was analyzed. For the 30 main pyrolysis products (Table S2), the bonds that are characteristic of these structures have been identified and the percentage of the total content of each component has been calculated based on peak areas (Table S3). Figure 4 shows the relative area normalization of some phenolic pyrolysis products for each lignin sample. Only those compounds are shown that are most significantly affected by the delignification method.

Lignin preparations were conditionally divided into three groups: near-native (MWL, DL); moderately modified (SodaEt-L, DMSO-L); and highly modified (Kraft-L, Soda-L, Hyd-L), depending on the amount of pyrolysis products. DL and SodaEt-L released volatiles in similar or slightly higher amounts compared to MWL (line “total peak area” in Table S2). In contrast, highly modified lignins released much less volatile pyrolysis products. Hyd-L produced 7 times less volatile compounds than MWL. A correlation was found between the type of lignin and the peak areas of various classes of organic compounds (Table 3).

Thus, MWL tends to produce alkenes, aldehydes, and alcohols, but not ketones or other non-radicals structural units. DL does not tend to produce hydroxyphenyl- or guaiacyl-types products. Instead, it tends to be syringyl-types compounds. Regarding radicals, DL tends to produce aldehydes and alcohols, rather than non-radical compounds and ketone.

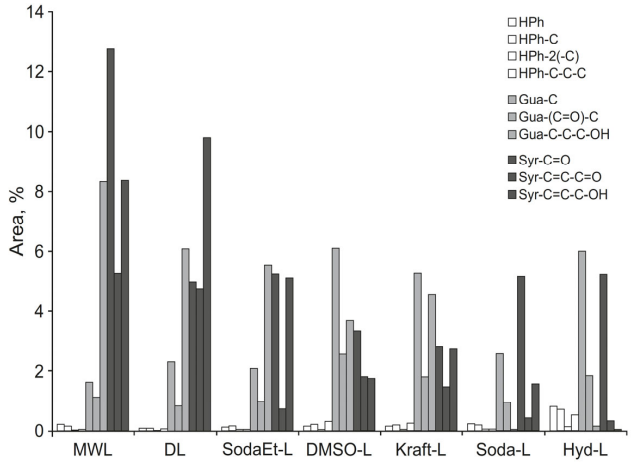

Fig. 4. The relative area of selected pyrolysis products.

SodaEt-L is also prone to produce alkenes, aldehydes, and alcohols, but not alkanes or ketones.

Soda-L is prone to release p-hydroxyphenyl-type products, but not alcohols and syringyls with a long-chain radicals. Regarding radicals–without radicals, or with alkane, alkene, or aldehyde.

Kraft-L is prone to release non-radicals structural units, alkanes and ketones, but not aldehydes.

DMSO-L tends to produce alkanes and ketones with different carbon chain lengths (from 1 to 3 C-atoms), but not aldehydes or alcohols.

Hyd-L is prone to release non-radicals structural units, alkanes and ketones, but not alcohols and aldehydes.

Near-native lignins are characterized by an increased content of alkenes, aldehydes and alcohols, and a smaller amount of non-radical products, alkanes, and ketones. DL contains a relatively high amount of syringyls and long-chain radicals.

A reduced content of aldehydes and alcohols characterizes highly modified lignins, as well as a high amount of non-radical structural units, alkanes and ketones. Mild isolation conditions preserve double C-C bonds, aldehyde and alcohol groups, preventing their cleavage and formation of non-radical products, alkane or ketone groups. On the other hand, harsh isolation conditions can lead to the breaking of C=C bonds, the oxidation of aldehydes and alcohols into ketones, alkanes formation, or losing a radical.

RDBEs of the studied lignins are shown in Fig. 5. The RDBE for the entire lignin preparation indicate a higher amount of unsaturated bonds in near-native lignins (MWL, DL) and a lower amount in highly modified lignins (DMSO-L, Soda-L, Kraft-L, Hyd-L, SodaEt-L).

RDBE vs C_n diagrams (Fig. S1) allowed us to divide the lignins under study into two groups. The first group included MWL and DL, characterized by many heavy unsaturated molecules (RDBE 5-6 and Cn 10-11). The second group includes highly modified lignins (DMSO-L, Soda-L, Kraft-L, Hyd-L), characterized by a smaller number of compounds with RDBE 5 and 6. Based on the features of the RDBE-charts in the second group, two subgroups can be identified – SodaEt-L and Soda-L are in one group, and DMSO-L, Kraft-L and Hyd-L are in the other.

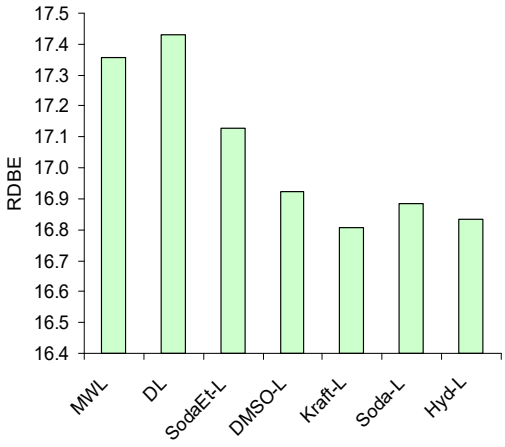

Fig. 5. RDBE of the studied lignins.

Table 3. The percentage of different classes of pyrolysis products of lignin isolated by various methods

	MWL	DL	SodaEt-L	DMSO-L	Kraft-L	Soda-L	Hyd-L
Non-radical	16.5 ± 0.2	18.9 ± 0.9	13.0 ± 0.8	25.9 ± 0.9	20.83 ±0.9	18.2 ± 0.8	21.1 ± 0.9
Alkanes	52.5 ± 0.6	51.4 ± 0.9	55.4 ± 0.9	49.6 ± 0.9	52.9 ± 0.9	58.4 ± 0.9	60.5 ± 0.9
Alkenes	31.0 ± 0.9	29.8 ± 0.8	31.6 ± 2.6	24.5 ± 0.6	26.2 ± 0.8	23.5 ± 0.9	18.4 ± 0.5
Aldehydes	25.3 ± 0.8	18.2 ± 0.7	18.2 ± 0.9	17.9 ± 0.2	7.1 ± 0.5	8.3 ± 0.6	9.9 ± 0.1
Ketones	12.3 ± 0.4	14.4 ± 0.9	20.8 ± 0.9	13.6 ± 0.4	20.4 ± 1.0	25.2 ± 0.9	26.2 ± 0.6
Alcohols	16.7 ± 0.9	10.7 ± 0.7	15.9 ± 0.9	1.6 ± 0.2	7.2 ± 0.1	5.4 ± 0.6	0.19 ± 0.02

Based on the elemental composition of the pyrolysis products defined in Table S2, the ratios of H/C and O/C were calculated and van Krevelen diagrams were constructed. Using van Krevelen diagrams, the general trends in lignin structure changes in different isolation methods were assessed [30-33]. For this purpose, lines of dehydration/condensation reactions (±H_2O), demethoxylation (±CH_2O), and alkyl chain length change (±CH_2) were constructed on the basis of syringol molecule (molecular formula $C_8H_{10}O_3$). This allowed us to calculate the H/C and O/C values for these compounds (Table S4). The obtained values were used to calculate the coefficients a and b of the linear approximation (2) in the van Krevelen coordinates.

$$y = ax + b \quad (2)$$

where y – H/C; x – O/C; a and b – constants of each reaction type (Table S4, Fig. 6).

The displacement along the solid line (Fig. 6) towards the lower left corner of the diagram is associated with water elimination processes (dehydration/condensation reactions). The shift along the dash-dotted line down to the left is associated with demethoxylation reactions (elimination of CH_2O). Moving down the dotted line to the right corresponds to a reduction in the alkyl chain length (elimination of –CH_2–), and the distribution of data points along this axis shows a variety of homologues with different alkyl chain length.

Figure 7 shows the van Krevelen diagrams of pyrolysis products for low-modified (near-native) lignin preparation (a) and the most modified (b). The pyrolysis products of lignins on the van Krevelen diagrams (Fig. 7, Fig. S2) occupy a region with O/C 0.2–0.5 and H/C 1.0–1.4 that is characteristic of lignin. The area of pyrolysis products of low-modified MWL sample stretches along the line of homologues (±CH_2). At the same time, this area is compressed along the reaction lines of demethoxylation and dehydration. Such distribution of methoxyl groups correlates with the natural abundance of phenol, guaiacol, and syringol homologues in lignin. For lignin preparations isolated under harsh conditions, the pyrolysis products are stretched along the lines of methoxyl groups and water elimination, and compressed along the homologues (±CH_2) line, which reflects the processes that occur under harsh isolation conditions – dehydration, polymerization, and demethoxylation.

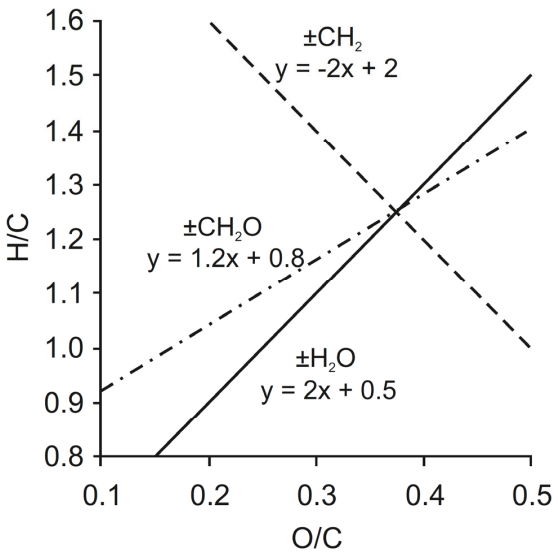

Fig. 6. The result of modeling reaction lines on the van Krevelen diagram.

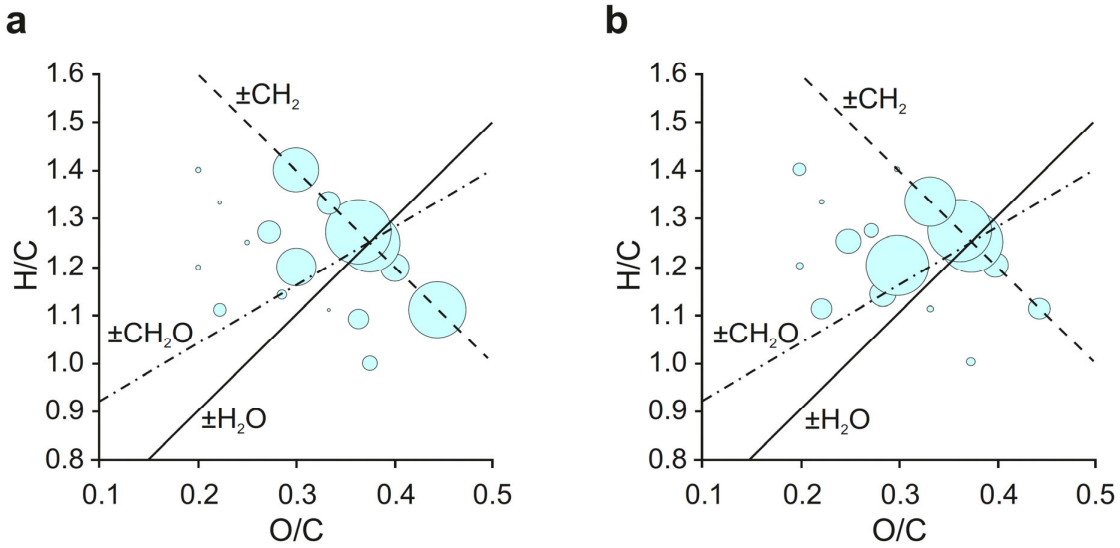

Fig. 7. van Krevelen diagrams for MWL (a) and Hyd-L (b) pyrolysis products.

3.2 Chemometric analysis

Differences in the structure of lignins, depending on the method of delignification, were visualized using principal component analysis (PCA) and hierarchical cluster analysis (HCA) of the contribution of 27 individual pyrolysis products to the S-, G-, and H-type structures (Table S3).

3.2.1 Hierarchical cluster analysis (HCA)

According to the dendrogram obtained (Fig. 8), the studied samples have been grouped into two main clusters. The first cluster contains near-native lignins, which differ significantly from both the rest of the samples and from each other (similarity less than 30%). This indicates a wide variety of structures in the MWL and DL samples. The second cluster contains lignins with a more limited variety of structures, due to the harsher isolation conditions used. This cluster is divided into two subclusters: the first subcluster contains SodaEt-L and Soda-L samples with an average variety of structures (similarity less than 50%). Kraft-L, DMSO-L and Hyd-L were included in the second subcluster, indicating that these samples underwent the most degradation during the delignification process and have the least structural diversity.

3.2.2 Principal component analysis (PCA)

The variations in the data can be described by 6 principal components (Fig. S3), 4 of which account for 96% of the total differences (PC1 – 40.99%; PC2 – 30.70%; PC3 – 12.79%; PC4 – 11.48%). Therefore, 4 is the optimal number of components to take into consideration. The contribution of the fragments to the overall difference was analyzed for each of the 4 components and presented in Table S5.

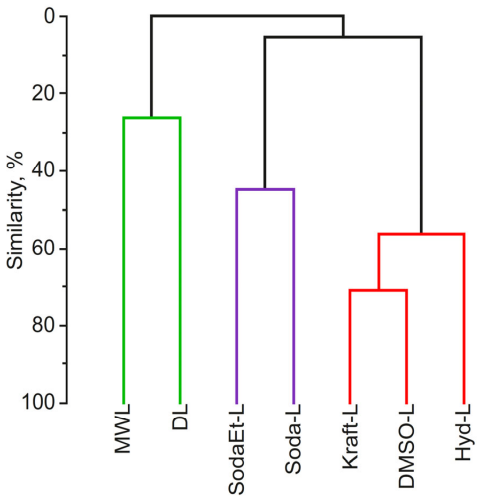

Fig. 8. Dendrogram obtained by hierarchical cluster analysis of lignin pyrolysis products.

Score plot of PC2 versus PC1 (PC2/PC1) helps to reveal the main trends in structural variability. On the left side of the graph, there is a predominance of unsaturated compounds and aldehydes. On the right side, there is a predominance of saturated compounds and ketones. Score plot of PC4 versus PC3 (PC4/PC3), in contrast, allows to focus on more subtle differences in structure, while ignoring the main differences.

The distribution of PC2/PC1 variations (Fig. 9a) divided the studied samples into 3 main groups.

The first group (Fig. 9a, green circles) included MWL and DL samples. The predominance of Gua C=O, Gua-C-C-C-OH, Syr-C=O, Syr-C=C-C=O, Syr-C=C-C-OH, and Syr-C-C=C are responsible for such differentiation. Considering the more subtle differences on the PC4/PC3 score plot (Fig. 9b), it is noteworthy that MWL is characterized by an increased content of HPh-C-C, Gua-C=O, Syr-C=O, and Syr C=C-C=O. While the DL sample is similar in subtle differences to SodaEt-L, which are characterized by an increased content of Syr-C-(C=O)-C, Syr-C-C=O, Gua-C-(C=O)-C, Gua-C-C-C, and Syr-C=C-C-OH.

The second PC2/PC1 group (Fig. 9a, purple circles) included SodaEt-L and Soda-L samples. These samples are characterized by a high content of Gua-C-C-C, Syr-C=C, and Syr-C-C=O. According to PC4/PC3, the Soda-L sample is characterized by an increased content of Gua, Gua-C, Gua-C-C, Syr, and Syr-C-C.

The third PC2/PC1 group (Fig. 9a, red circles) consisted of Kraft-L, DMSO-L, Hyd-L, which are characterized by the predominance of HPh-C-C-C, Gua-C, Gua-(C=O)-C, Syr-C, Syr-C-(C=O)-C-, and Syr-(C=O)-C. In subtle differences, the Kraft-L and DMSO-L samples are very similar, they are characterized by an increased content of Gua-C-C, Gua-(C=O)-C, Gua-C-C=C, and Syr.

Special attention should be paid to the Hyd-L sample, as it has a separate location on both score plots. According to the distribution of PC2/PC1 variations, this sample is characterized by an increased HPh, HPh-C, HPh-2(-C), HPh-C-C, HPh-C-C-C, Gua, Gua-C, Gua-C=C, Gua-C-(C=O)-C, Syr, and Syr-C-(C=O)-C content. The increased content of Syr-(C=O)-C-C and HPh-2(-C) is responsible for the separate location of this sample on the score plot of PC4/PC3.

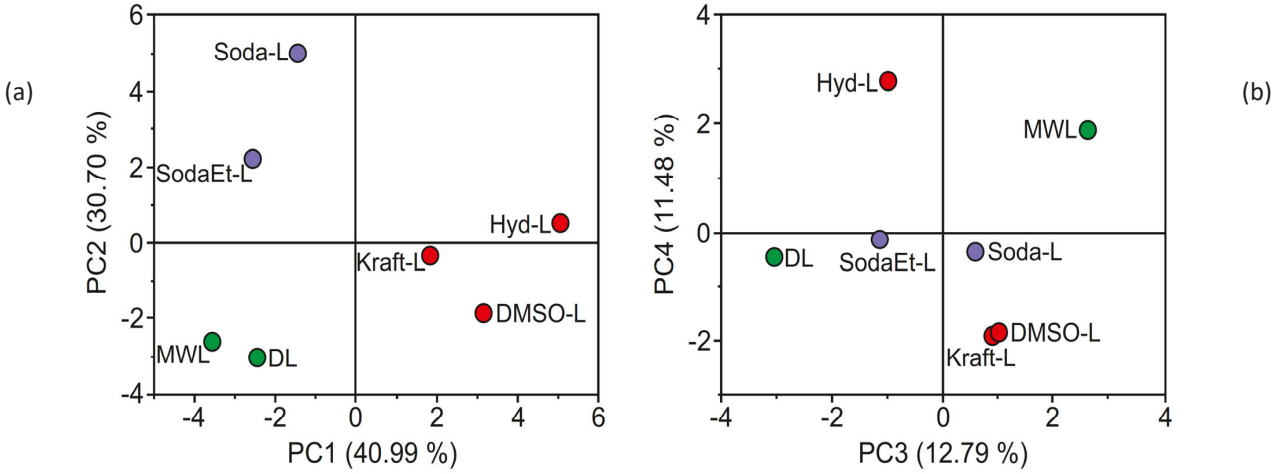

Fig. 9. Score plots of PC2/PC1 (a) and PC4/PC3 (b), obtained by PCA analysis of pyrolysis products of various lignins.

4. Conclusions

The monomeric composition of technical and near-native birch lignins during pyrolytic decomposition has been studied. The studied lignins were obtained by various methods of both mild delignification (milled wood lignin – MWL, dioxane lignin – DL) and harsh delignification processes (alkaline ethanol lignin – SodaEt-L, soda lignin – Soda-L, dimethyl sulfoxide lignin – DMSO-L, sulfate/kraft lignin – Kraft-L, and hydrolysis lignin – Hyd-L), some of them are widely used in P&P industry.

The contribution of the main monomeric units (S/G/H) to the lignin macromolecule was evaluated. Structural fragments are shown, the content of which is significantly influenced by the method of lignin extraction. The difference in the relative amounts of pyrolysis products of various lignins is shown. Hyd-L released 7 times less volatiles then MWL. Near-native lignins are characterized by an increased content of alkenes, aldehydes and alcohols, as well as a decreased amount of non-radical products, alkanes and ketones.

The use of RDBE vs C_n and van Krevelen diagrams allowed to comprehensively characterize the monomeric composition of lignin pyrolysis products. Thus, the MWL sample was characterized by a wide variety of bonds, and a large amount of oxygen and double bonds in the composition of the molecule. Samples of highly modified lignins were characterized by a smaller number of homologues and fewer double bonds and oxygen atoms.

Hierarchical cluster analysis (HCA) allowed to divide studied lignins into three distinct groups: low-modified/near-native (MWL, DL); moderately modified (SodaEt-L, Soda-L); and highly modified (Kraft-L, DMSO-L, Hyd-L). At the same time, the similarity between the near-native samples was less than 30%, which indicates a structural variability of lignins. The samples from the third group had the least variety of structures.

Differences in the structure of lignins, depending on the method of delignification, were visualized using principal component analysis (PCA). According to the score plot of PC2/PC1, it was determined that the structures of unsaturated compounds and aldehydes, as well as saturated compounds and ketones, contribute most significantly to the difference between the samples. The score plot of PC4/PC3 showed more subtle differences in the structure of lignins. Hyd-L differs significantly from other studied samples and undergoes the most significant structural changes during the delignification process.

Based on this study, mathematical modeling of delignification processes is possible. The investigation can form the basis for upgrading delignification and pyrolysis methods, increasing the efficiency and environmental safety of the processes.

The work complements existing studies in the field of thermal treatment of lignin, expanding knowledge about the effect of process parameters on decomposition products.

The results of the work can be used in industry for different strategies of lignin processing. Obtaining information on how various industrial delignification methods affect the composition and amount of monomeric pyrolysis products allow optimizing technological processes into more efficient and targeted ones.

The data obtained can be used to create new types of fuel, carbon materials or chemicals with improved characteristics. Understanding the dependence of

lignin destruction and modification on specific delignification methods allow optimizing processing technologies that increase the yield of valuable products during pyrolysis (with an emphasis on reducing the negative environmental impact).

Acknowledgments

This research was performed using an instrumentation of the Core Facility Center "Arktika" of the Northern (Arctic) Federal University named after M.V. Lomonosov.

Funding

This research was funded by the Ministry of Science and Higher Education of the Russian Federation (state assignment project No. FSRU-2024-0003).

Supplementary material

Supplementary data to this article can be found online at: https://doi.org/10.18321/ectj1661

References

[1]. A.V. Faleva, A.Y. Kozhevnikov, S.A. Pokryshkin, et al., Structural characteristics of different softwood lignins according to 1D and 2D NMR spectroscopy, *J. Wood Chem. Technol.* 40 (2020) 1–15. DOI: 10.1080/02773813.2020.1722702

[2]. C. Heitner, D. Dimmel, J. Schmidt, Advances in chemistry, in: Lignin and Lignans, CRC Press, 2016. DOI: 10.1201/EBK1574444865

[3]. R. Vanholme, K. Morreel, J. Ralph, W. Boerjan, Lignin engineering, *Curr. Opin. Plant Biol.* 11 (2008) 278–285. DOI: 10.1016/j.pbi.2008.03.005

[4]. D.S. Bajwa, G. Pourhashem, A.H. Ullah, S.G. Bajwa, A concise review of current lignin production, applications, products and their environmental impact, *Ind. Crops Prod.* 139 (2019) 111526. DOI: 10.1016/j.indcrop.2019.111526

[5]. F.G. Calvo-Flores, J.A. Dobado, J. Isac-García, F.J. Martín-Martínez, Lignin and Lignans as Renewable Raw Materials: Chemistry, Technology and Applications, John Wiley & Sons, 2015. DOI: 10.1002/9781118682784

[6]. H. Chen, Lignocellulose Biorefinery Engineering: Feedstock Engineering, Academic Press, 2015. DOI: 10.1016/B978-0-08-100135-6.00003-X

[7]. D. Shen, G. Liu, J. Zhao, et al., Thermo-chemical conversion of lignin to aromatic compounds: Effect of lignin source and reaction temperature, *J. Anal. Appl. Pyrolysis* 112 (2015) 56–65. DOI: 10.1016/j.jaap.2015.02.022

[8]. I. Haq, P. Mazumder, A.S. Kalamdhad, Recent advances in removal of lignin from paper industry wastewater and its industrial applications, *Bioresour. Technol.* 305 (2020) 123636. DOI: 10.1016/j.biortech.2020.123636

[9]. Y. Ma, X. Ouyang, L. Zhao, et al., Catalytic conversion of lignin in birch sawdust into aromatic monomers over Co/CN catalyst under lignin first strategy, *Fuel* 363 (2024) 132203. DOI: 10.1016/j.fuel.2024.132203

[10]. H. Tan, P. Zhang, X. Geng, et al., Visible light-driven selective cleavage of Cα-Cβ or Cβ-O bond in lignin β-O-4 model into high-value aromatic chemicals over surface modified 2D g-C_3N_4, *Sep. Purif. Technol.* 352 (2024) 128765. DOI: 10.1016/j.seppur.2024.128765

[11]. A.Yu. Kozhevnikov, S.L. Shestakov, Yu.A. Sypalova, Functional composition and structural features of higher plant lignins, *Lesnoy Zhurnal* 5 (2023) 164–183. DOI: 10.37482/0536-1036-2023-5-164-183

[12]. A. Björkman, Studies on finely divided wood. Part 3. Extraction of lignin with neutral solvents, Svensk Papperstidning 59 (1956) 477–485.

[13]. A. Guerra, I. Filpponen, L.A. Lucia, D.S. Argyropoulos, Comparative evaluation of three lignin isolation protocols for various wood species, *J. Agric. Food Chem*. 54 (2006) 5939–5947. DOI: 10.1021/jf062433c

[14]. F.H.B. Sosa, D.O. Abranches, A.M. da Costa Lopes, et al., Role of deep eutectic solvent precursors as hydrotropes: Unveiling synergism and antagonism for enhanced kraft lignin dissolution, *ACS Sustain. Chem. Eng.* 12 (2024). DOI: 10.1021/acssuschemeng.4c02529

[15]. R.C. Sun, Lignin source and structural characterization, *ChemSusChem* 13 (2020) 1–12. DOI: 10.1002/cssc.202001324

[16]. E.M. Anderson, M.L. Stone, R. Katahira, et al., Differences in S/G ratio in natural poplar variants do not predict catalytic depolymerization monomer yields, *Nat. Commun.* 10 (2019) 1999. DOI: 10.1038/s41467-019-09986-1

[17]. A. Kumar, B. Biswas, K. Saini, et al., Py-GC/MS study of prot lignin with cobalt impregnated titania, ceria and zirconia catalysts, *Renew. Energy* 174 (2021) 458–468. DOI: 10.1016/j.renene.2021.03.011

[18]. D.G. Branco, C. Santiago, A. Lourenço, et al., Structural features of cork dioxane lignin from Quercus suber L., *J. Agric. Food Chem.* 69 (2021) 9329–9339. DOI: 10.1021/acs.jafc.1c01961

[19]. J. Rencoret, A. Gutiérrez, G. Marques, et al., New insights on structures forming the lignin-like fractions of ancestral plants, *Front. Plant Sci.* 12 (2021) 740923. DOI: 10.3389/fpls.2021.740923

[20]. F.J.F. Lopes, F.O. Silvério, D.C.F. Baffa, et al., Determination of sugarcane bagasse lignin S/G/H ratio by pyrolysis GC/MS, *J. Wood Chem. Technol.* 31 (2011) 309–323. DOI: 10.1080/02773813.2010.550379

[21]. S. Pokryshkin, Y. Sypalova, A. Ivahnov, A. Kozhevnikov, Optimization of approaches to analysis of lignin by thermal decomposition, *Polymers* 15 (2023) 2861. DOI: 10.3390/polym15132861

[22]. Y. Yang, Y. Ma, S. Yang, et al., Chemical components analysis of Toona sinensis bark and wood by pyrolysis–gas chromatography–mass spectrometry, *Asia-Pac. J. Chem. Eng*. 15 (2020) e2487. DOI: 10.1002/apj.2487

[23]. A. Ivahnov, Yu. Sypalova, S. Pokryshkin, A. Kozhevnikov, Organosolv delignification of birch wood (Betula pendula): DMSO/water pulping optimization, *Holzforschung* 76 (2022) 1–10. DOI: 10.1515/hf-2022-0113

[24]. L. Eriksson, Introduction to Multi- and Megavariate Data Analysis Using Projection Methods (PCA & PLS), Umetrics AB, 1999.

[25]. A.V. Faleva, I.A. Grishanovich, N.V. Ul'yanovskii, D.S. Kosyakov, Application of 2D NMR spectroscopy in combination with chemometric tools for classification of natural lignins, *Int. J. Mol. Sci.* 24 (2023) 12403. DOI: 10.3390/ijms241512403

[26]. E.E. Harris, E. Beglinger, G.J. Hajny, E.C. Sherrard, Hydrolysis of wood: treatment with sulfuric acid in a stationary digester, *Ind. Eng. Chem*. 37 (1945) 390–396. DOI: 10.1021/ie50421a005

[27]. X. Erdocia, F. Hernández-Ramos, A. Morales, et al., Lignin extraction and isolation methods, in: Lignin-Based Materials for Biomedical Applications, Elsevier, 2021, pp. 77–101. DOI: 10.1016/B978-0-12-820303-3.00004-7

[28]. E. Korotkova, A. Pranovich, J. Wärnå, et al., Lignin isolation from spruce wood with low concentration aqueous alkali at high temperature and pressure: influence of hot-water pre-extraction, *Green Chem.* 17 (2015) 5031–5042. DOI: 10.1039/C5GC01341K

[29]. A.K. Jain, M.N. Murty, P.J. Flynn, Data clustering: a review, *ACM Comput. Surv.* 31 (1999) 264–323. DOI: 10.1145/331499.331500

[30]. T.H. Trinh, Y. Uemura, A theoretical equation presenting slope in van Krevelen diagram for biomass pyrolysis, *Platform: A J. Eng.* 3 (2019) 46–65. DOI: 10.61762/pajevol3iss1art4665

[31]. M.F. Li, L.X. Chen, X. Li, et al., Evaluation of the structure and fuel properties of lignocelluloses through carbon dioxide torrefaction, *Energy Convers. Manag.* 122 (2016) 71–79. DOI: 10.1016/j.enconman.2016.04.064

[32]. S. Kim, R.W. Kramer, P.G. Hatcher, Graphical method for analysis of ultrahigh-resolution broadband mass spectra of natural organic matter, the van Krevelen diagram, *Anal. Chem.* 75 (2003) 5336–5344. DOI: 10.1021/ac034415p

[33]. D.C.P. Lozano, H.E. Jones, T.R. Reina, et al., Unlocking the potential of biofuels: via reaction pathways in van Krevelen diagrams, *Green Chem*. 23 (2021) 5744–5753. DOI: 10.1039/d1gc01796a